

Study of $V_L V_L \rightarrow t\bar{t}$ at the International Linear Collider including $\mathcal{O}(\alpha_s)$ QCD corrections

 Stephen Godfrey^{1,*} and Shou-hua Zhu^{1,2}
¹*Ottawa-Carleton Institute for Physics, Department of Physics, Carleton University, Ottawa, Canada K1S 5B6*
²*Institute of Theoretical Physics, School of Physics, Peking University, Beijing 100871, China*

(Received 24 December 2004; published 12 October 2005)

In the event that the Higgs mass is large or that the electroweak interactions are strongly interacting at high energy, top-quark couplings to longitudinal components of the weak gauge bosons could offer important clues to the underlying dynamics. It has been suggested that precision measurements of $W_L W_L \rightarrow t\bar{t}$ and $Z_L Z_L \rightarrow t\bar{t}$ might provide hints of new physics. In this paper we present results for $\mathcal{O}(\alpha_s)$ QCD corrections to $V_L V_L \rightarrow t\bar{t}$ scattering at the International Linear Collider (ILC). We find that corrections to cross sections can be as large as 30% and must be accounted for in any precision measurement of $VV \rightarrow t\bar{t}$.

 DOI: [10.1103/PhysRevD.72.074011](https://doi.org/10.1103/PhysRevD.72.074011)

PACS numbers: 12.38.Bx, 14.65.Ha, 12.60.-i, 14.80.Bn

I. INTRODUCTION

Understanding the mechanism of electroweak symmetry breaking (EWSB) is a primary goal of the large hadron collider (LHC) [1]. Numerous possibilities have been proposed and in some cases their experimental signatures have been studied in detail [2]. The models can be roughly divided into two scenarios. The first possibility is a weakly interacting weak sector which implies light Higgs bosons and naturally leads to supersymmetry which predicts many new supersymmetric particles [3]. The alternative scenario is a strongly interacting Higgs sector (SIWS) [4] most often described by dynamical symmetry breaking [5]. Recently, additional new approaches to EWSB have emerged, such as the little Higgs model [6–11] which contain ingredients from both scenarios and other alternative approaches such as “Higgsless” models [12–14]. Although the light Higgs mass scenario is favored by precision electroweak fits, models with heavy Higgs bosons can be accommodated by the data [15–17]. It is this latter possibility that we wish to study.

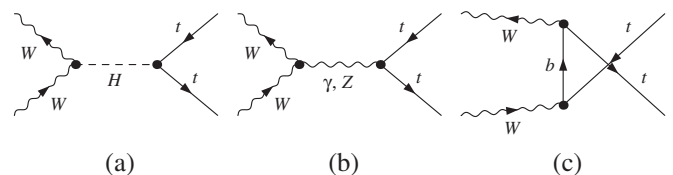
While the signature for the weakly interacting weak sector is the production of light Higgs bosons and possibly additional particles and many of the newer models predict relatively light extra gauge bosons, the signal for a SIWS will almost certainly be more subtle [18]. In the SIWS scenario W -boson interactions can be described by an effective Lagrangian with the coefficients in L_{eff} constrained by experiment [19]. Detailed studies have been made for the LHC [4,20–22].

Because the t -quark mass is the same order of magnitude as the scale of EWSB it has long been suspected that t -quark properties may provide hints about the nature of EWSB [23–29]. To this end studies have been performed of $VV \rightarrow t\bar{t}$ both in terms of the sensitivity to M_H [30–32], and in terms of an effective Lagrangian describing vector boson t -quark interactions [33]. Moreover, this process should be sensitive to models such as top-color [34] and

the top seesaw model [35]. Because of the Goldstone boson equivalence theorem [36] the longitudinal gauge bosons (W_L^\pm, Z_L) are equivalent to the Goldstone modes at energies much larger than their mass so that they reflect the properties of EWSB. In principle, $V_L V_L \rightarrow t\bar{t}$ can be studied at both hadron colliders through $q_1 q_2 \rightarrow q'_1 q'_2 V_L V'_L$ and at high energy $e^+ e^-$ colliders via $e^+ e^- \rightarrow \ell_1 \ell_2 V_L V'_L$ or $\gamma\gamma \rightarrow V_L V'_L + X$ [24,30–32,37]. While the LHC will be the first high energy collider to explore the TeV energy region the overwhelming QCD backgrounds for $t\bar{t}$ production will likely make it impossible to study the $V_L V_L \rightarrow t\bar{t}$ subprocess [38].

The International Linear Collider (ILC) offers a much cleaner environment to study the $V_L V_L \rightarrow t\bar{t}$ subprocess. The simplest approach is to study how the $t\bar{t}$ cross section varies with M_H . This has been studied by several authors [30–32]. The tree-level Feynman diagrams for the SM process are given in Fig. 1. The $e^+ e^- \rightarrow \nu\bar{\nu}t\bar{t}$ cross section is shown as a function of M_H in Fig. 2 for an $e^+ e^-$ collider with center of mass energy $\sqrt{s}_{e^+e^-} = 1$ TeV. We convoluted the effective W approximation (EWA) distributions [39,40] with the $W_L^+ W_L^- \rightarrow t\bar{t}$ cross section to obtain the $e^+ e^- \rightarrow \nu\bar{\nu}t\bar{t}$ cross sections and included the kinematic cuts $M_{t\bar{t}} > 400$ GeV and $p_T^{t\bar{t}} > 10$ GeV. The values for these kinematic cuts were chosen so that in the former case the EWA is reasonably reliable and in the latter case to reduce various backgrounds. This is discussed more fully in Sec. IV.

A more general approach is to parametrize interactions in a nonlinearly realized electroweak chiral Lagrangian [19] which is appropriate if the EWSB dynamics is strong


 FIG. 1. The tree-level diagrams for $W^+ W^- \rightarrow t\bar{t}$.

 *Email address: godfrey@physics.carleton.ca

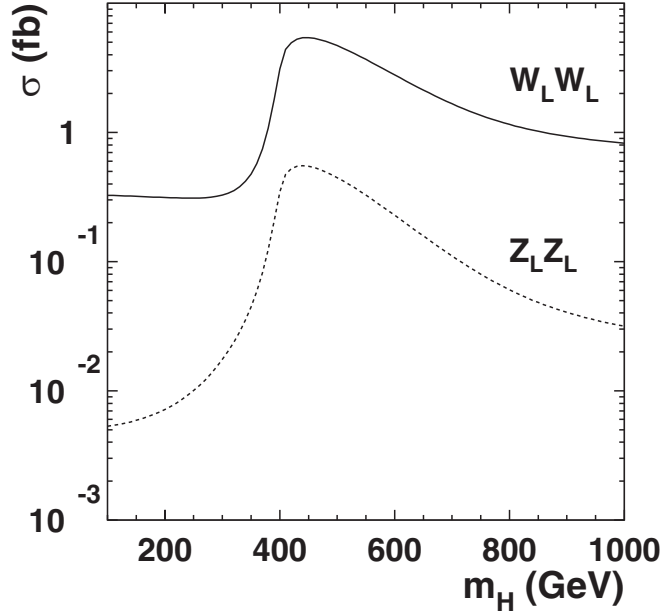


FIG. 2. The solid line is for $\sigma(e^+e^- \rightarrow \nu\bar{\nu}t\bar{t})$ (the $W_L^+W_L^- \rightarrow t\bar{t}$ subprocess) and the dotted line is for $\sigma(e^+e^- \rightarrow e^+e^-t\bar{t})$ (the $Z_L Z_L \rightarrow t\bar{t}$ subprocess) as a function of M_H for an e^+e^- collider with center of mass energy $\sqrt{s}_{e^+e^-} = 1$ TeV and kinematic cuts $m_{t\bar{t}} > 400$ GeV and $p_T^{t,\bar{t}} > 10$ GeV.

with no Higgs bosons at low energies. For illustrative purposes we show the sensitivity of the cross sections to a representative dimension five operator;

$$L_1^{\text{eff}} = \frac{a_1}{\Lambda} \bar{t}t W_\mu^+ W^{-\mu}, \quad (1)$$

where the coefficient a_1 is naively expected to be of order 1 when the cutoff of the theory is taken to be $\Lambda = 4\pi v = 3.1$ TeV with $v = 246$ GeV, the vacuum expectation value of the SM Higgs field. We do not rigorously follow the chiral Lagrangian approach and simply include the operator of Eq. (1) as an additional $WWt\bar{t}$ interaction. The effect of varying a_1 for an e^+e^- collider with $\sqrt{s}_{e^+e^-} = 1$ TeV is shown in Fig. 3 using the EWA and the same kinematic cuts as before. $\sigma(e^+e^- \rightarrow \nu\bar{\nu}t\bar{t})$ is shown for $M_H = 120$, 500, and 1000 GeV and for $M_H = \infty$. The latter case is referred to in the literature as the ‘‘low energy theorem’’ (LET) model. A careful analysis by Ref. [33,41] finds that the $V_L V_L t\bar{t}$ coupling can be measured to an accuracy of $\sim \pm 0.1$ at 95% C.L. (with the cutoff scale of $\Lambda = 3.1$ TeV divided out as expressed in Eq. (1)).

These approaches are complementary to studies based on specific models and on the linear realization of EW symmetry breaking which includes physical Higgs bosons in the particle spectrum. The crucial point is that precision measurements of top-quark interactions could play an important role in understanding the mechanism of EWSB. But to be able to attach meaning to precision measurements it is necessary to understand radiative corrections, both electroweak and QCD.

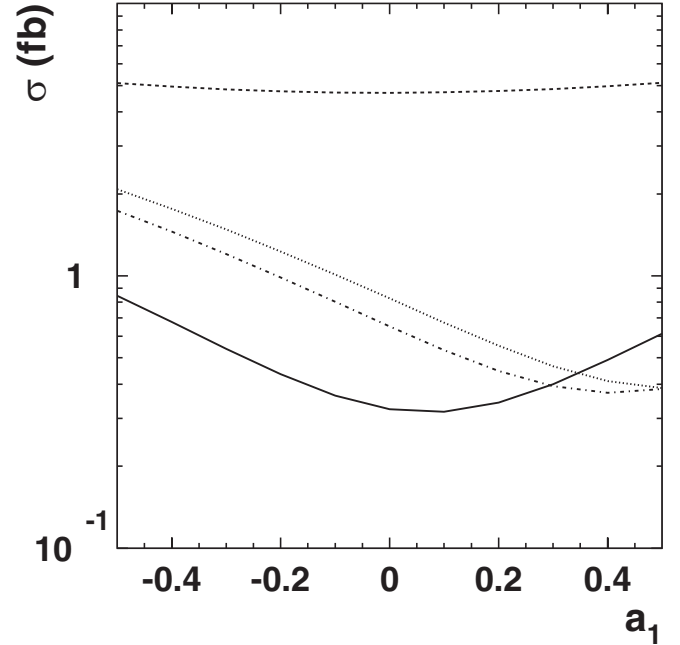


FIG. 3. $\sigma(e^+e^- \rightarrow \nu\bar{\nu}t\bar{t})$ (the $W_L^+W_L^- \rightarrow t\bar{t}$ subprocess) vs the $WWt\bar{t}$ coupling a_1 for $\sqrt{s}_{e^+e^-} = 1$ TeV with the same kinematic cuts as Fig. 2. The solid line is for $M_H = 120$ GeV, the dashed line for $M_H = 500$ GeV, the dotted line for $M_H = 1$ TeV, and the dashed-dotted line for $M_H = \infty$ (the LET scenario).

In this paper we quantify the importance of QCD radiative corrections for the process $V_L V_L \rightarrow t\bar{t}$. We focus on the $\mathcal{O}(\alpha_s)$ QCD corrections to the tree level electroweak $V_L V_L \rightarrow t\bar{t}$ process in the SM at the ILC. We begin in Sec. II by summarizing the effective W approximation and how it is implemented in our calculations. The bulk of the section is devoted to how we calculated the QCD corrections. Numerical results are given in Sec. III with Sec. IV devoted to a discussion of other aspects which should be considered in a complete calculation of $t\bar{t}$ production. Concluding comments are given in the final section.

II. CALCULATIONS

We are interested in the subprocesses $VV \rightarrow t\bar{t}$ which occur in the processes

$$e^+e^- \rightarrow \ell_1\ell_2 + VV \rightarrow \ell_1\ell_2 + t\bar{t}, \quad (2)$$

where $\ell_1\ell_2$ is $\nu\bar{\nu}$ for the $W^+W^- \rightarrow t\bar{t}$ subprocess and e^+e^- for the $ZZ \rightarrow t\bar{t}$ subprocess. Before proceeding to the QCD corrections we briefly summarize the effective vector boson approximation (EVA).

A. The effective vector boson approximation

In the effective vector boson approximation the W and Z bosons are treated as partons inside the electron [39,40]. The total cross section is then obtained by integrating the

W (of Z) luminosities with the subprocess cross section [37].

$$\sigma(e^+e^- \rightarrow \ell_1 \ell_2 t\bar{t}) = \sum_{\lambda_1, \lambda_2} \int_{\hat{s}/m_{t\bar{t}}^2}^1 d\tau \frac{d\mathcal{L}}{d\tau} \hat{\sigma}(V_{\lambda_1} V_{\lambda_2} \rightarrow t\bar{t}) \quad (3)$$

where λ_1 and λ_2 are the V 's polarization, $\tau = \hat{s}/s$ with s and \hat{s} the e^+e^- and VV center-of-mass energy, respectively, and \mathcal{L} is the $V_{\lambda_1} V_{\lambda_2}$ luminosity given by

$$\frac{d\mathcal{L}}{d\tau} = \int_{\tau}^1 \frac{dx}{x} f_{V_{\lambda_1}/e}(x) f_{V_{\lambda_2}/e}(\tau/x). \quad (4)$$

The $f_{V/e}$ distributions are given by [39,40]

$$f_{V_{\pm}/e}(x) = \frac{C}{16\pi^2 x} [(g_V^f \mp g_A^f)^2 + (g_V^f \pm g_A^f)^2 (1-x)^2] \times \log\left(\frac{4E^2}{M_V^2}\right) \quad (5)$$

$$f_{V_L/e}(x) = C \frac{(g_V^f)^2 + (g_A^f)^2}{4\pi^2} \left[\frac{1-x}{x} \right] \quad (6)$$

for the transverse and longitudinal V 's, respectively, and where for a W boson $C = g^2/8$, $g_V = -g_A = 1$, and for a Z boson $C = g^2/\cos^2\theta_w$, $g_V = \frac{1}{2}T_3 - Q\sin^2\theta_w$, $g_A = -\frac{1}{2}T_3$ with g the coupling constant for the weak-isospin group $SU(2)_L$ and E the energy of the initial lepton. With these expressions for the V distributions, the luminosity for LL scattering simplifies to [39,40]:

$$\frac{d\mathcal{L}_{LL}}{d\tau} = \frac{[(g_V^e)^2 + (g_A^e)^2]^2}{16\pi^4 \tau} [2(\tau-1) - (1+\tau)\log\tau]. \quad (7)$$

B. $\mathcal{O}(\alpha_s)$ corrections to $VV \rightarrow t\bar{t}$

We next describe how we calculated the $\mathcal{O}(\alpha_s)$ corrections for the process $W^+W^- \rightarrow t\bar{t}$. The results for $ZZ \rightarrow t\bar{t}$ are obtained the same way. To obtain our results we used the FEYNARTS, FORMCALC, and LOOPTOOLS packages [42]. We point out details specific to our calculation but refer the interested reader to the descriptions of the packages for further information.

The tree-level Feynman diagrams for $W^+W^- \rightarrow t\bar{t}$ are given in Fig. 1 and the virtual diagrams are shown in Fig. 4(a). The infrared singularity in the vertex corrections are cancelled by the soft contributions from the process $W^+W^- \rightarrow t\bar{t}g$ which are shown in Fig. 4(b). Since only soft photon formulas are embedded in the FEYNARTS/FORMCALC/LOOPTOOLS packages, to accommodate the soft gluons we modified the corresponding formulas with the substitution $eQ \rightarrow g_s T_a$. For processes with no triple-gluon vertex present, introducing a gluon mass is equivalent to standard dimensional regularization. Introducing a small finite gluon mass is easily included using the pack-

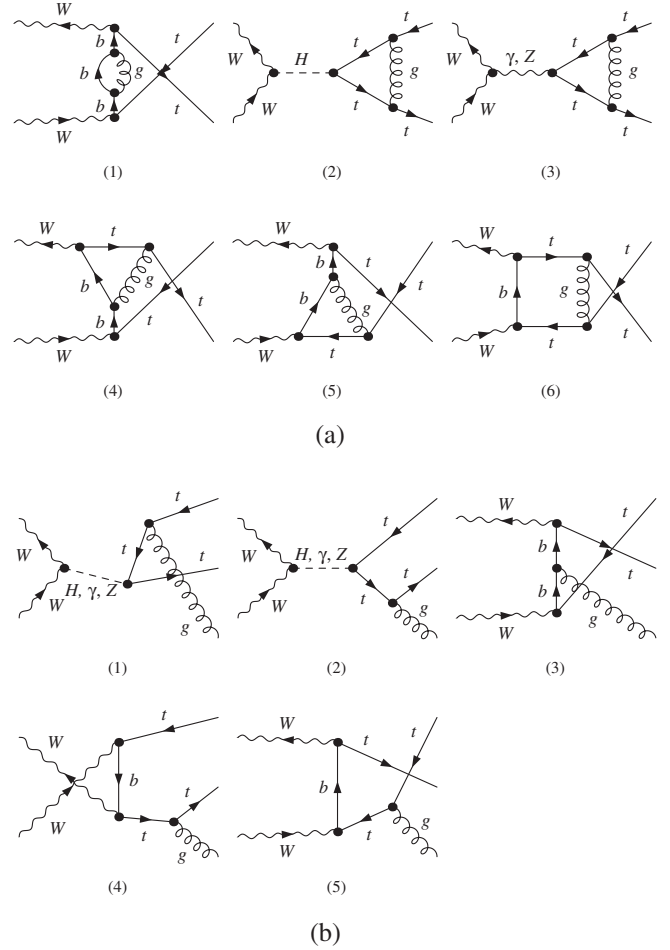


FIG. 4. $\mathcal{O}(\alpha_s)$ QCD corrections to $W^+W^- \rightarrow t\bar{t}$. (a) Virtual QCD contributions to $W^+W^- \rightarrow t\bar{t}$. (b) Feynman diagrams for $W^+W^- \rightarrow t\bar{t}g$.

ages we employ, so for convenience we regulate the IR-singularity this way. This approach has the additional benefit that varying the value of the gluon mass acts as a check of the numerical cancellations between the different contributions.

The cross sections are calculated by replacing the Born matrix element squared by

$$|M_{\text{Born}}|^2 \rightarrow |M_{\text{Born}}|^2 (1 + \delta_{\text{soft}}) + 2 \text{Re}(M_{\text{Born}}^* \delta M), \quad (8)$$

where δM is the sum of the one-loop Feynman diagrams and the corresponding counter-term diagrams and δ_{soft} is the soft-gluon correction factor coming from the $2 \rightarrow 3$ process. The hard contribution from the $2 \rightarrow 3$ process is also $\mathcal{O}(\alpha_s)$ and will be discussed further below. Thus, Eq. (8) yields the cross section including all $\mathcal{O}(\alpha_s)$ corrections but neglects the $\mathcal{O}(\alpha_s^2)$ corrections that are included in the dropped $|\delta M|^2$ contribution.

To deal with renormalization associated with the ultraviolet divergences we adopt the on-mass shell renormalization scheme and use dimensional regularization. In the on-mass shell renormalization scheme for the external

quark legs, the top-quark self-energy is cancelled by its corresponding counter-term. For this reason we do not explicitly show the top-quark self-energy diagrams in Fig. 4. The scale dependence in this calculation only enters in α_s and we take it to be \hat{s} . We will discuss uncertainties due to this choice below.

The software packages we used handle renormalization by employing numerical factors. For example, the UV divergence is represented by a numerical factor Δ . Because our results must be independent of these factors we can vary them to check the consistency of our results. In particular, the UV finiteness is checked by verifying the independence of the results to Δ and in the on-mass shell renormalization scheme to the dimensional regularization scale parameter μ .

As mentioned above, the IR-singularity was regulated by introducing a finite gluon mass which is allowed when no triple-gluon vertex contributes to the amplitude. The cancellation of the finite gluon contributions from the vertex correction with the soft-gluon production in $W^+W^- \rightarrow t\bar{t}g$ is a strong test of the veracity of our results. We performed this check and also verified that the results are independent of the gluon regulator mass but for the sake of brevity do not show plots of these results.

A final check is to verify that the results are independent of the soft cutoff energy of the emitted gluon which divides the cross section into a piece with a soft gluon emitted and a piece with a hard gluon emitted. To do so we sum the results of the hard $WW \rightarrow t\bar{t}g$ process with the soft $WW \rightarrow t\bar{t}g$ plus 1-loop results. While individually the hard and soft pieces are dependent on the soft cutoff energy of the emitted gluon, the sum will not be. We have checked that our results are indeed independent of the gluon cutoff energy.

To obtain cross sections from the analytical results for the squared amplitudes, the FORMCALC package integrates phase space using Gaussian quadrature for the 2 to 2 process and the VEGAS Monte Carlo integration package for the 2 to 3 process.

III. RESULTS

In Fig. 5 we show the tree-level electroweak and $\mathcal{O}(\alpha_s)$ QCD corrected cross sections for the subprocesses $W^+W^- \rightarrow t\bar{t}$ and $ZZ \rightarrow t\bar{t}$ for a Higgs boson mass of 500 GeV and for all W and Z polarizations. In all cases we include the $t\bar{t} + g$ final state in the $\mathcal{O}(\alpha_s)$ results. To separate out the hard gluon case depends on details of the detector and the jet finding algorithms which is beyond the scope of this paper. As before, we include in these and all subsequent results the kinematic cuts $m_{t\bar{t}} > 400$ GeV and $p_T^{t,\bar{t}} > 10$ GeV. The Born results agree with previous results [30]. The longitudinal scattering cross section is much larger than the TT and TL cases. Since it is the longitudinal gauge boson processes which corresponds to the Goldstone bosons of the theory we will henceforth only include

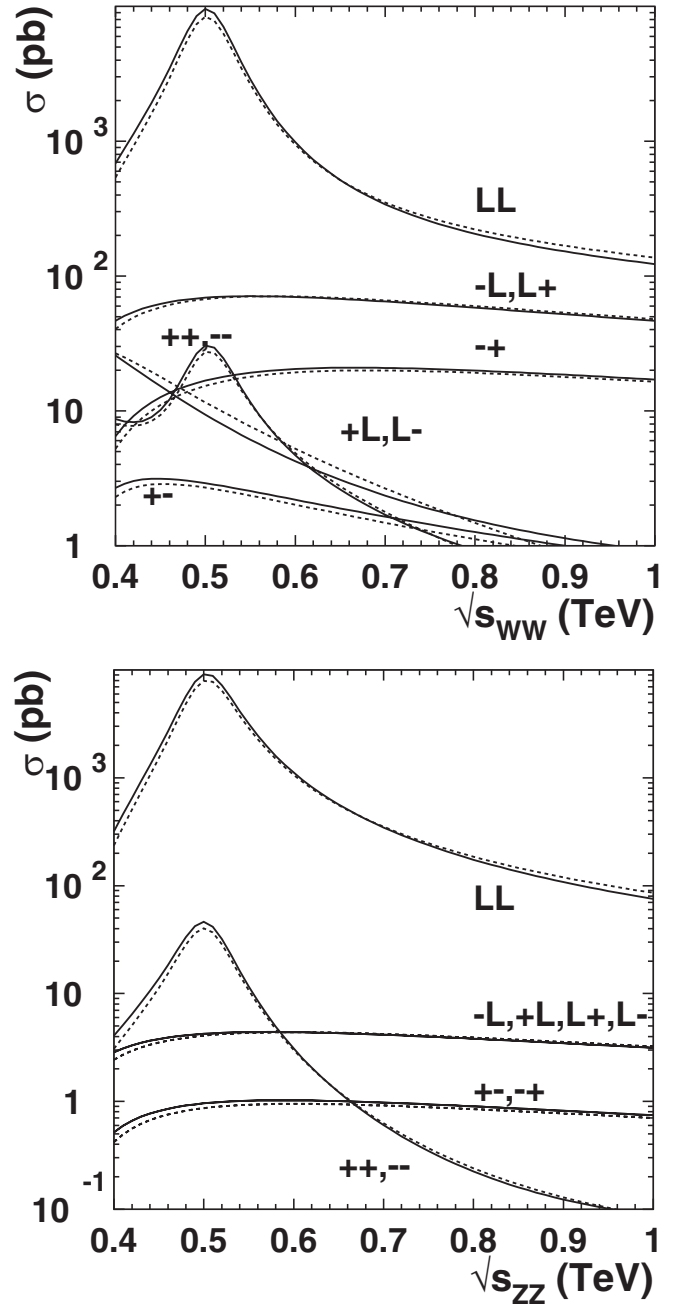


FIG. 5. Cross sections as a function of $\sqrt{\hat{s}}$ for the subprocesses (a) $W^+W^- \rightarrow t\bar{t}$ and (b) $ZZ \rightarrow t\bar{t}$. In both cases $m_H = 500$ GeV for the $\mathcal{O}(\alpha_s)$ QCD corrected (solid) and electroweak tree level (dashed).

results for $V_L V_L$ scattering. In Fig. 6 we show the cross section only including longitudinal W and Z scattering as a function of the e^+e^- center of mass energy for several representative Higgs masses including the $M_H \rightarrow \infty$ case (corresponding to the LET).

The QCD corrections to longitudinal scattering are often presented as a K -factor, normally defined as the ratio of the NLO to LO cross sections. Because the $\mathcal{O}(\alpha_s)$ QCD corrections we have calculated in this paper are LO correc-

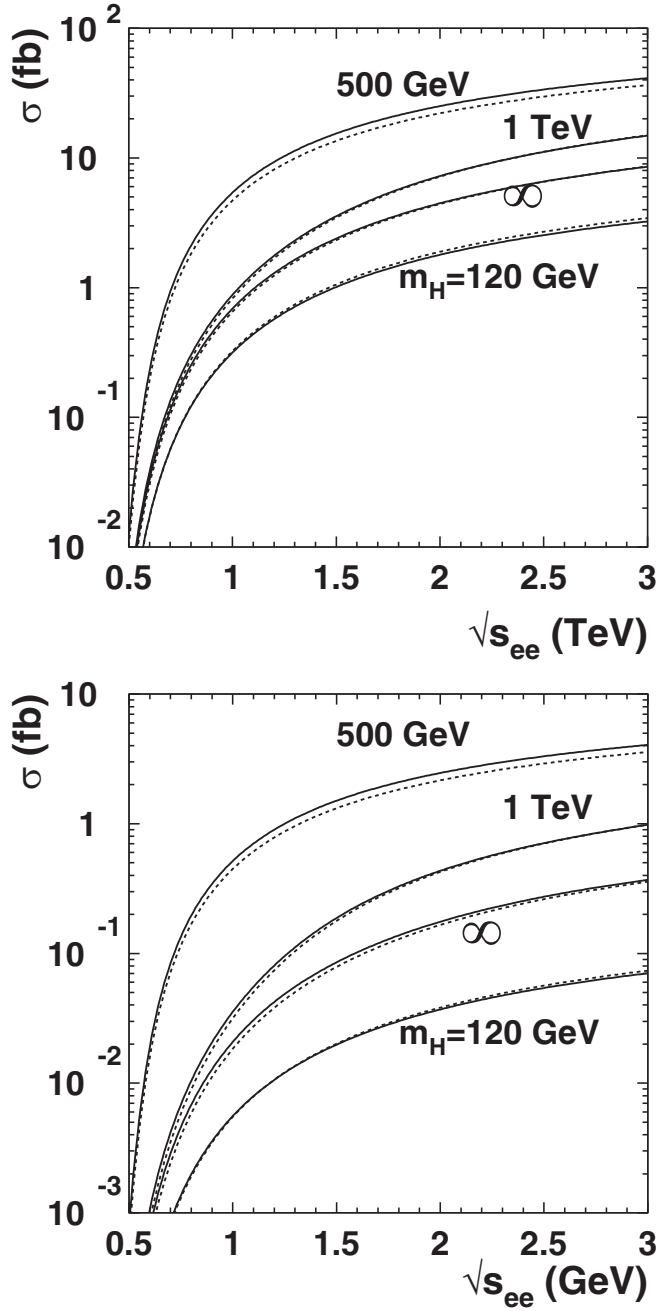


FIG. 6. Cross sections as a function of $\sqrt{s_{e^+e^-}}$ for (a) $e^+e^- \rightarrow \nu\bar{\nu}t\bar{t}$ via $W_L^+W_L^-$ fusion and for (b) $e^+e^- \rightarrow e^+e^-t\bar{t}$ via $Z_L Z_L$ fusion. In both cases the solid line is the $\mathcal{O}(\alpha_s)$ QCD corrected cross section and the dashed line is the electroweak tree-level cross section.

tions to a tree-level electroweak result we are taking the K -factor to be the ratio of the cross section with the $\mathcal{O}(\alpha_s)$ QCD corrections and the tree-level electroweak cross sections. The K -factors for $\sigma(e^+e^- \rightarrow \nu\bar{\nu}t\bar{t})$ which goes via $W_L^+W_L^-$ fusion and for $\sigma(e^+e^- \rightarrow e^+e^-t\bar{t})$ which goes via $Z_L Z_L$ fusion are shown in Fig. 7 as a function of the e^+e^- center of mass energy. K -factors are shown for $M_H = 120$ GeV, 500 GeV, 1 TeV, and the LET case (using the

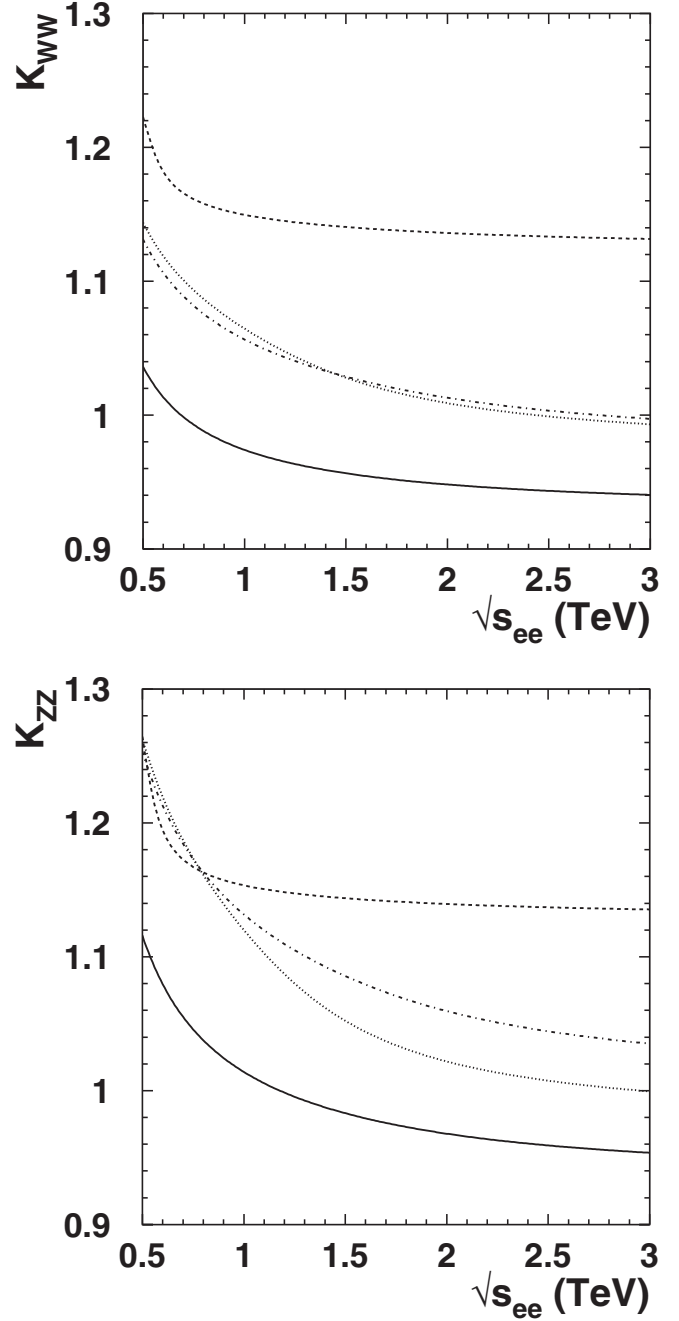


FIG. 7. The K -factors as a function of $\sqrt{s_{e^+e^-}}$ for (a) $e^+e^- \rightarrow \nu\bar{\nu}t\bar{t}$ (via $W_L^+W_L^-$ fusion) and for (b) $e^+e^- \rightarrow e^+e^-t\bar{t}$ (via $Z_L Z_L$ fusion). In both cases the solid line is for $M_H = 120$ GeV, the dashed line for $M_H = 500$ GeV, the dotted line for $M_H = 1$ TeV, and the dot-dashed line for $M_H = \infty$ (LET). See text for an explanation of the K -factor.

same kinematic cuts as before). The $\mathcal{O}(\alpha_s)$ QCD corrections are largest for $M_H = 500$ GeV with K -factors ranging from over 1.2 for $\sqrt{s_{e^+e^-}} = 500$ GeV to 1.15 for $\sqrt{s_{e^+e^-}} = 1$ TeV. The corrections decrease as the e^+e^- center-of-mass energy increases. The corrections are smallest for a light Higgs but in that case we will probably study top-Higgs couplings in other processes such as asso-

ciated top-Higgs production. As can be seen from Fig. 7 the $M_H = 1$ TeV and LET cases lie between these two extremes. The variation of the K -factor with M_H is shown more explicitly in Fig. 8. The fact that the K -factor is largest for $M_H = 500$ GeV in Fig. 7 and that it peaks at $M_H \simeq 400$ GeV in Fig. 8 is a threshold effect which is an artifact of the kinematic cut we imposed on the $t\bar{t}$ invariant mass. When we pass through the kinematic threshold the

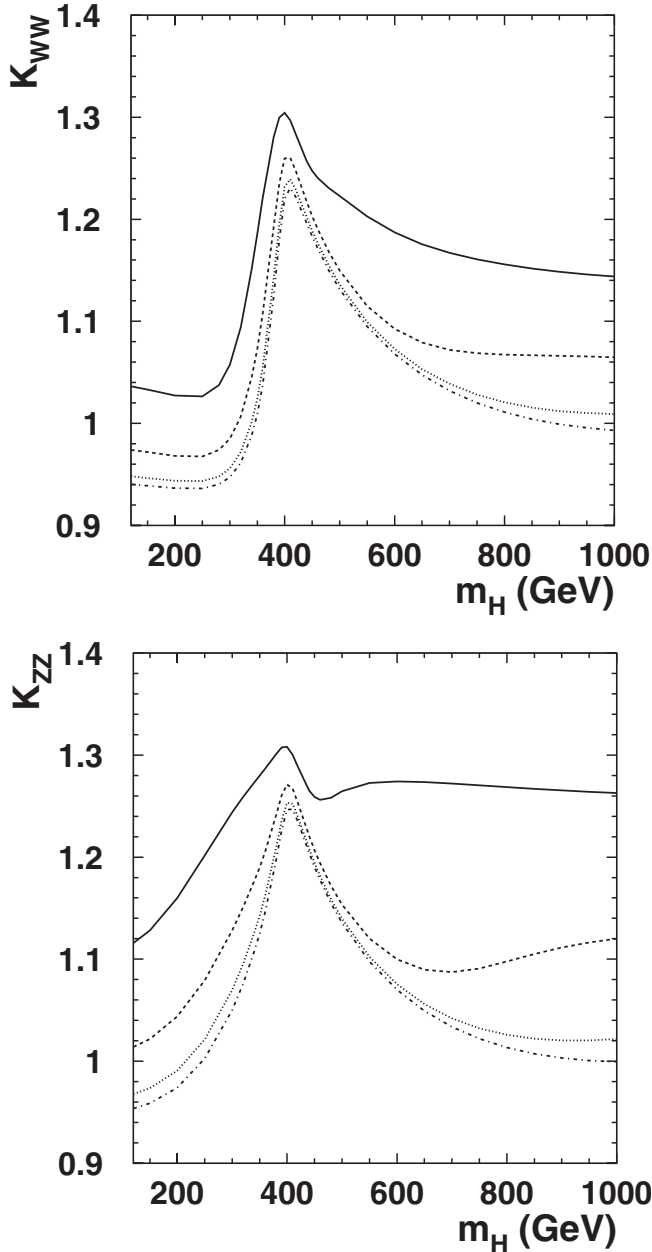


FIG. 8. The K -factor as a function of M_H for (a) $e^+e^- \rightarrow \nu\bar{\nu}t\bar{t}$ (via $W_L^+W_L^-$ fusion) and for (b) $e^+e^- \rightarrow e^+e^-t\bar{t}$ (via Z_LZ_L fusion). In both cases the solid line is for $\sqrt{s}_{e^+e^-} = 500$ GeV, the dashed line for $\sqrt{s}_{e^+e^-} = 1$ TeV, the dotted line for $\sqrt{s}_{e^+e^-} = 2$ TeV, and the dot-dashed line for $\sqrt{s}_{e^+e^-} = 3$ TeV. See text for an explanation of the K -factor.

dominant contribution to the $t\bar{t}$ threshold comes from the s -channel Higgs resonance. This threshold behavior is also seen in Fig. 3 of Ref. [30] but at a different value of M_H reflecting the different $M_{t\bar{t}}^{\text{cut}}$ used in that paper. This threshold region also corresponds to a region of low Q^2 relevant to soft-gluon emission resulting in larger QCD corrections. As the phase space opens up the QCD corrections are expected to decrease which is what is observed. One also sees in Fig. 8 how the K -factor decreases as $\sqrt{s}_{e^+e^-}$ increases. The important point one comes away with from Fig. 7 and 8 is that it is clear that QCD corrections are not insignificant compared to the effects we might wish to study such as top Yukawa couplings or anomalous $VVt\bar{t}$ couplings.

A brief comment about uncertainties due to scale dependence is in order. As stated above, the scale dependence in this calculation only enters in α_s which we took to be \hat{s} . To estimate uncertainties due to scale dependence we vary the scale by a factor of 2 smaller and a factor of 2 larger at the peak in the subprocess, $\hat{\sigma}$, which is the dominant contribution to the e^+e^- cross sections. We find an uncertainty of $\sim 15\%$ in α_s which leads to at most $\sim 4\%$ uncertainty in the K -factor.

IV. DISCUSSION

In this paper we concentrated on $\mathcal{O}(\alpha_s)$ QCD corrections. There are equally important considerations and contributions that we have neglected. For completeness we briefly describe them here.

Backgrounds are always an important ingredient and have been discussed in Ref. [4,28,32]. Briefly, the relevant signal is a $t\bar{t}$ pair with missing transverse momentum carried by the neutrinos or from the beam electrons not observed by the detector. The largest background is direct $t\bar{t}$ production. It can be suppressed by requiring missing mass greater than some minimum value. This background can be further reduced by choosing the jet association that best reconstructs the t and W masses. Another significant background is $t\bar{t}$ production via other gauge boson fusion with the largest being $\gamma\gamma \rightarrow t\bar{t}$ [37]. This can be reduced by requiring the missing transverse energy to be greater than some value, with a value of 50 GeV used by Alcaraz and Morales for a TeV collider [32]. The final background we mention is $e^+e^- \rightarrow \gamma t\bar{t}$ where the photon escapes the detector but is sufficiently hard to generate the required p_T . Most of this background can be eliminated with an appropriate cut on the p_T^{eff} of the $t\bar{t}$ pair [41]. Additionally the signal could be enhanced using polarized beams [41].

At present the electroweak radiative corrections for top-quark production have not been calculated and there are ambiguities which still need to be better understood. In general, when the Higgs boson mass is heavy, the electroweak correction to the process contains the enhancement factor $\alpha m_H^2/M_W^2$ which will be significant. However, S -matrix elements of $VV \rightarrow t\bar{t}$ are not well-defined for

unstable external particles so are problematic for higher-order calculations that include the Higgs width at the born level. The discussion of this issue has been given for the process $W^+W^- \rightarrow W^+W^-$ in [43]. The full process with stable initial and final particles needs to be considered if one includes electroweak corrections consistently. This is beyond the scope of this paper.

The accuracy of the effective W approximation has been studied by a number of authors. Assuming a cut on the invariant mass of $M_{t\bar{t}} > 500$ GeV the resulting cross sections typically agree to about 10% with the exact calculation [41]. This is the same order of magnitude as the effects we are interested in measuring and the QCD corrections considered in this paper. Therefore, an exact calculation would be required for precision measurements of $t\bar{t}$ cross sections.

Finally, we mention that the subprocess $W^+W^- \rightarrow t\bar{t}$ is also possible in $\gamma\gamma$ collisions but the standard model direct processes overwhelm this subprocess by several orders of magnitude. Analogous to the e^+e^- case one can use the effective W luminosity inside photons [44,45]. It is possible that judicious choices of kinematic cuts could enhance the signal; in $\gamma\gamma \rightarrow t\bar{t}$ the cross section is dominated by the top-quarks collinear to the beam while in the W -fusion process the spectator W 's along the beam direction could be used to tag events [44]. We leave this process for a future study.

V. CONCLUSIONS

In the event that the Higgs mass is heavy and the electroweak sector is strongly interacting it is quite possible that the underlying theory will manifest itself in the interactions between the top quark and longitudinal component of gauge bosons. Different aspects of this have been studied but the common theme is that precision measurements at a future high energy e^+e^- would be necessary to understand the underlying dynamics. In this paper we studied the $\mathcal{O}(\alpha_s)$ QCD corrections to the tree-level electroweak process $VV \rightarrow t\bar{t}$. We found that they can be quite substantial, the same size as the effects we wish to study, so that they need to be taken into account when studying $t\bar{t}$ production. Although the kinematic cuts that are chosen will change the numerical results slightly, the $\mathcal{O}(\alpha_s)$ QCD corrections are understood and should not pose a barrier in studying these processes.

ACKNOWLEDGMENTS

S. G. thanks Frank Petriello for helpful discussions. This research was supported in part by the Natural Sciences and Engineering Research Council of Canada. S.Z. was also supported in part by the Natural Science Foundation of China under Grant No. 90403004.

-
- [1] For a recent review, see R. Barbieri, in *Proceedings of the Cargèse School of Particle Physics and Cosmology: the Interface, Cargèse, Cosica, France, 2003*, NATO Science Series II: Mathematics, Physics and Chemistry Vol. 188, edited by D. Kazakov and G. Smadja (Springer, Dordrecht, 2005), p. 517; hep-ph/0312253.
 - [2] Atlas Collaboration, “*ATLAS Detector and Physics Performance*,” Technical Design Report No. CERN-LHCC-99-15, Vol. 2.
 - [3] H. Baer *et al.*, hep-ph/9503479.
 - [4] T. L. Barklow *et al.*, in *Proceedings of the 1996 DPF/DPB Summer Study on New Directions on High-Energy Physics (Snowmass 96)*, Snowmass, CO, 1996, edited by D. G. Cassel, L. Trindle Gennari, and R. H. Siemann, eConf C960625, STC118 (1996) p. 735; hep-ph/9704217.
 - [5] C. T. Hill and E. H. Simmons, Phys. Rep. **381**, 235 (2003); **390**, 553 (2004).
 - [6] N. Arkani-Hamed, A. G. Cohen, and H. Georgi, Phys. Lett. B **513**, 232 (2001); N. Arkani-Hamed, A. G. Cohen, T. Gregoire, and J. G. Wacker, J. High Energy Phys. 08 (2002) 020; N. Arkani-Hamed, A. G. Cohen, E. Katz, A. E. Nelson, T. Gregoire, and J. G. Wacker, J. High Energy Phys. 08 (2002) 021; N. Arkani-Hamed, A. G. Cohen, E. Katz, and A. E. Nelson, J. High Energy Phys. 07 (2002) 034.
 - [7] I. Low, W. Skiba, and D. Smith, Phys. Rev. D **66**, 072001 (2002).
 - [8] For a recent review see M. Schmaltz, Nucl. Phys. B Proc. Suppl. **117**, 40 (2003).
 - [9] T. Han, H. E. Logan, B. McElrath, and L. T. Wang, Phys. Rev. D **67**, 095004 (2003).
 - [10] J. L. Hewett, F. J. Petriello, and T. G. Rizzo, J. High Energy Phys. 10 (2003) 062.
 - [11] M. Perelstein, M. E. Peskin, and A. Pierce, Phys. Rev. D **69**, 075002 (2004).
 - [12] C. Csaki, C. Grojean, H. Murayama, L. Pilo, and J. Terning, Phys. Rev. D **69**, 055006 (2004).
 - [13] C. Csaki, C. Grojean, L. Pilo, and J. Terning, Phys. Rev. Lett. **92**, 101802 (2004).
 - [14] H. Davoudiasl, J. L. Hewett, B. Lillie, and T. G. Rizzo, Phys. Rev. D **70**, 015006 (2004).
 - [15] M. E. Peskin and J. D. Wells, Phys. Rev. D **64**, 093003 (2001).
 - [16] M. S. Chanowitz, Phys. Rev. D **66**, 073002 (2002).
 - [17] R. Barbieri, A. Pomarol, R. Rattazzi, and A. Strumia, Nucl. Phys. **B703**, 127 (2004).
 - [18] A recent account of these topics is given in LHC/LC Study Group, “*Physics Interplay of the LHC and the ILC*,” hep-ph/0410364.
 - [19] S. Dawson and G. Valencia, Nucl. Phys. **B352**, 27 (1991);

- A. Dobado, M.J. Herrero, and J. Terron, *Z. Phys. C* **50**, 205 (1991).
- [20] M. S. Chanowitz, hep-ph/9812215.
- [21] R. Rosenfeld and J.L. Rosner, *Phys. Rev. D* **38**, 1530 (1988).
- [22] J. Bagger *et al.*, *Phys. Rev. D* **49**, 1246 (1994); J. Bagger *et al.*, *Phys. Rev. D* **52**, 3878 (1995).
- [23] M. S. Chanowitz, M. A. Furman, and I. Hinchliffe, *Nucl. Phys.* **B153**, 402 (1979).
- [24] F. Larios and C. P. Yuan, *Phys. Rev. D* **55**, 7218 (1997).
- [25] X. Zhang, S. K. Lee, K. Whisnant, and B. L. Young, *Phys. Rev. D* **50**, 7042 (1994).
- [26] K. Whisnant, B. L. Young, and X. Zhang, *Phys. Rev. D* **52**, 3115 (1995).
- [27] J. Wudka, hep-ph/9706434.
- [28] T. Han, Y. J. Kim, A. Likhoded, and G. Valencia, *Nucl. Phys.* **B593**, 415 (2001).
- [29] T. Han, G. Valencia, and Y. Wang, *Phys. Rev. D* **70**, 034002 (2004).
- [30] M. Gintner and S. Godfrey, hep-ph/9612342;
- [31] E. Ruiz Morales and M. E. Peskin, hep-ph/9909383.
- [32] J. Alcaraz and E. Ruiz Morales, *Phys. Rev. Lett.* **86**, 3726 (2001).
- [33] F. Larios, T. M. P. Tait, and C. P. Yuan, hep-ph/0101253.
- [34] C. T. Hill, *Phys. Lett. B* **266**, 419 (1991); See also C. T. Hill *et al.* (Ref. [5]) for a recent review.
- [35] B. A. Dobrescu and C. T. Hill, *Phys. Rev. Lett.* **81**, 2634 (1998); R. S. Chivukula, B. A. Dobrescu, H. Georgi, and C. T. Hill, *Phys. Rev. D* **59**, 075003 (1999).
- [36] B. W. Lee, C. Quigg, and H. B. Thacker, *Phys. Rev. D* **16**, 1519 (1977); M. S. Chanowitz and M. K. Gaillard, *Nucl. Phys.* **B261**, 379 (1985); Y. P. Yao and C. P. Yuan, *Phys. Rev. D* **38**, 2237 (1988); J. Bagger and C. Schmidt, *Phys. Rev. D* **41**, 264 (1990); H. G. J. Veltman, *Phys. Rev. D* **41**, 2294 (1990); H. J. He, Y. P. Kuang, and X. Y. Li, *Phys. Rev. Lett.* **69**, 2619 (1992); H. J. He and W. B. Kilgore, *Phys. Rev. D* **55**, 1515 (1997).
- [37] R. P. Kauffman, *Phys. Rev. D* **41**, 3343 (1990).
- [38] T. Han, D. L. Rainwater, and G. Valencia, *Phys. Rev. D* **68**, 015003 (2003).
- [39] R. Cahn and S. Dawson, *Phys. Lett. B* **136**, 196 (1984); **138**, 464E (1984); S. Dawson, *Nucl. Phys.* **B249**, 42 (1985); M. Chanowitz and M. Gaillard, *Phys. Lett. B* **142**, 85 (1984); G. Kane, W. Repko, and W. Rolnick, *Phys. Lett. B* **148**, 367 (1984); J. Lindfors, *Z. Phys. C* **28**, 427 (1985).
- [40] S. Dawson and S. S. D. Willenbrock, *Nucl. Phys.* **B284**, 449 (1987).
- [41] F. Larios, T. Tait, and C. P. Yuan, *Phys. Rev. D* **57**, 3106 (1998).
- [42] T. Hahn, *Nucl. Phys. B Proc. Suppl.* **89**, 231 (2000), and references therein.
- [43] A. Denner and T. Hahn, *Nucl. Phys.* **B525**, 27 (1998).
- [44] K. M. Cheung, *Phys. Rev. D* **50**, 4290 (1994).
- [45] K. Hagiwara, I. Watanabe, and P. M. Zerwas, *Phys. Lett. B* **278**, 187 (1992).